

1 **What Caused the Significant Increase in Atlantic Ocean Heat Content**  
2 **Since the mid-20th Century?**  
3  
4  
5  
6

7 Sang-Ki Lee<sup>1,2</sup>, Wonsun Park<sup>3</sup>, Erik van Sebille<sup>5</sup>, Molly Baringer<sup>2</sup>, Chunzai Wang<sup>2</sup>, David B.  
8 Enfield<sup>1,2</sup>, Steven Yeager<sup>4</sup>, and Ben Kirtman<sup>5</sup>

9 <sup>1</sup>Cooperative Institute for Marine and Atmospheric Studies, University of Miami, Miami,  
10 Florida, USA

11 <sup>2</sup>Atlantic Oceanographic and Meteorological Laboratory, NOAA, Miami Florida, USA

12 <sup>3</sup>Leibniz Institute of Marine Sciences (IFM-GEOMAR), Kiel, Germany

13 <sup>4</sup>National Center for Atmospheric Research, Boulder, Colorado, USA

14 <sup>5</sup>Rosenstiel School for Marine and Atmospheric Science, University of Miami, Miami, Florida,  
15 USA

16  
17 Revised to Geophysical Research Letters

18 July 2011  
19  
20  
21

22 Corresponding author address: Dr. Sang-Ki Lee, NOAA/AOML, 4301 Rickenbacker Causeway,  
23 Miami, FL 33149, USA. E-mail: [Sang-Ki.Lee@noaa.gov](mailto:Sang-Ki.Lee@noaa.gov).

1 **Abstract**

2 As the upper layer of the world ocean warms gradually during the 20th century, the inter-  
3 ocean heat transport from the Indian to Atlantic basin should be enhanced, and the Atlantic  
4 Ocean should therefore gain extra heat due to the increased upper ocean temperature of the  
5 inflow via the Agulhas leakage. Consistent with this hypothesis, instrumental records indicate  
6 that the Atlantic Ocean has warmed substantially more than any other ocean basin since the mid-  
7 20th century. A surface-forced global ocean-ice coupled model is used to test this hypothesis and  
8 to find that the observed warming trend of the Atlantic Ocean since the 1950s is largely due to an  
9 increase in the inter-ocean heat transport from the Indian Ocean. Further analysis reveals that the  
10 increased inter-ocean heat transport is not only caused by the increased upper ocean temperature  
11 of the inflow but also, and more strongly, by the increased Agulhas Current leakage, which is  
12 augmented by the strengthening of the wind stress curl over the South Atlantic and Indian  
13 subtropical gyre.

1 **1. Introduction**

2 Recently updated and bias-corrected instrumental records indicate that the heat content of the  
3 Atlantic Ocean in the upper 700 m has substantially increased during the 1970s – 2000s at a rate  
4 ( $\sim 2.0 \times 10^{22}$  J per decade) almost matching that of the Pacific Ocean ( $\sim 1.5 \times 10^{22}$  J per decade)  
5 and Indian Ocean ( $\sim 0.5 \times 10^{22}$  J per decade) combined [Levitus et al., 2009], even though the  
6 Atlantic Ocean covers less than 20% of the global ocean in surface area. Climate model  
7 experiments with and without anthropogenic greenhouse forcing have shown that the observed  
8 warming of the global ocean since the mid-20th century could be largely attributed to the  
9 anthropogenic greenhouse effect [Barnett et al. 2001; Levitus et al., 2001; Barnett et al. 2005].  
10 However, a question still remains as to why the warming trend in the Atlantic Ocean is  
11 substantially larger than that in other ocean basins. This is also an important question for our  
12 understanding of past, present and future climate variability on regional and global scales  
13 because, for instance, tropical precipitation and Atlantic hurricane activity in the 21st century  
14 could be affected by a differential inter-ocean warming [e.g., Lee et al., 2011].

15 Deep convective mixing over the North Atlantic sinking regions could cause the subpolar  
16 North Atlantic sea surface temperatures (SSTs) to become relatively insensitive to the  
17 anthropogenic greenhouse effect, and thus decreasing the longwave heat loss at the sea surface  
18 and increasing the radiative heating associated with anthropogenic greenhouse gases. However,  
19 this hypothesis appears to be inconsistent with the observed cooling trend of the subpolar North  
20 Atlantic Ocean in the upper 1500 m during the 1950s - 1990s [e.g., Lozier et al. 2010].

21 Perhaps, the answer to this conundrum can be found in the global overturning circulation, the  
22 large scale ocean circulation that connects the Pacific, Indian and Southern Oceans to deep  
23 convection in the North Atlantic sinking regions, carrying with it heat, freshwater and carbon, etc

1 [Broecker, 1987]. As the upper layer of the world ocean warms gradually, the inter-ocean heat  
2 transport via the global overturning circulation should increase given that the radiative heating  
3 associated with the anthropogenic greenhouse effect is more or less uniform over the world  
4 ocean [Palmer et al. 2007]. The increased inter-ocean heat transport should further warm the  
5 Atlantic Ocean since the Atlantic basin is characterized by advective heat convergence (i.e., the  
6 northward ocean heat transport at 30°S in the South Atlantic is always positive) due to the  
7 Atlantic Meridional Overturning Circulation (AMOC), which is the Atlantic component of the  
8 global overturning circulation. The Atlantic warming should continue until the deep layer of the  
9 Atlantic Ocean fully adjusts to the increased radiative heating over the world ocean and exports  
10 the warm water out of the basin at depth or until the AMOC weakens due to the increased  
11 buoyancy in the North Atlantic sinking regions. This hypothesis is in line with the results from  
12 Palmer and Haines [2009] who used historical hydrographic observations from 1970 to 2000 to  
13 make quantitative estimates of the contribution to ocean heat content changes from the ocean  
14 heat transport convergence (estimated by deepening of the reference isotherm of 14°C) versus  
15 surface heating (estimated by warming above the 14°C isotherm). They found that the ocean heat  
16 transport convergence dominates only in the Atlantic basin. Grist et al. [2010] used a high-  
17 resolution global ocean model forced with historical surface meteorological fields to find a  
18 consistent result.

19 Changes in the strength and spatial structure of the AMOC could also modulate the ocean  
20 heat transport convergence in the Atlantic basin, and thus may have contributed to the observed  
21 warming of the Atlantic Ocean since the mid-20th century. However, it is difficult to attribute  
22 the increased Atlantic Ocean heat content to AMOC variability because there is no reliable long-  
23 term instrumental record of the AMOC. It appears that an ocean model-based reconstruction is

1 likely to be our best chance for assessing the history of AMOC in the 20th century because the  
2 relatively long time series of estimated surface flux fields, which constrain ocean-ice coupled  
3 models, are available from atmospheric reanalysis products. Therefore, in the following sections,  
4 we use a series of global ocean-ice model simulations to explore why the Atlantic Ocean has  
5 warmed much more than any other ocean basin since the mid-20th century.

6

## 7 **2. 20th Century Reanalysis (20CR)**

8 The paucity of observational hydrographic data makes it a challenge for proper initialization  
9 a global model at the mid-20th century. An alternative approach is to start an ocean model  
10 simulation sufficiently earlier than the mid-20th century. This will finesse issues involving the  
11 model initialization. However, none of the surface-forced ocean model studies so far has been  
12 simulated with the surface forcing prior to the mid-20th century because the surface forcing data,  
13 which are typically derived from atmospheric reanalysis products, are limited to the last 50 - 60  
14 years. Recently, the newly developed NOAA-CIRES 20th Century Reanalysis (20CR) has been  
15 completed [Compo et al., 2010]. The 20CR provides the first estimate of global surface fluxes  
16 spanning the late 19th century and the entire 20th century (1871-2008) at daily temporal and 2°  
17 spatial resolutions.

18

## 19 **3. Model Experiments**

20 The global ocean-ice coupled model of the NCAR Community Climate System Model  
21 version 3 (CCSM3) forced with the 20CR is used as the primary tool in this study. The ocean  
22 model is divided into 40 vertical levels. Both the ocean and ice models have 320 longitudes and  
23 384 latitudes on a displaced pole grid with a longitudinal resolution of about 1.0 degrees and a

1 variable latitudinal resolution of approximately 0.3 degrees near the equator. See Doney et al.  
2 (2007) for more detailed descriptions about the CCSM3 ocean-ice model (CCSM3\_POP  
3 hereafter).

4 To spin up the model, a fully coupled (atmosphere-land-ocean-ice) CCSM3 control  
5 experiment is performed for 700 years with the pre-industrial climate condition of the 1870s. The  
6 700th year output of the CCSM3 spin-up run is then used to initialize the CCSM3\_POP, which is  
7 further integrated for 200 more years using the daily 20CR surface flux fields for the period of  
8 1871-1900. To incorporate the impact of atmospheric noise, which plays a crucial role in the  
9 thermohaline convection and deep-water formation in the North Atlantic sinking regions  
10 [personal communication with Ping Chang], during the spin-up the surface forcing fields in each  
11 model year are randomly selected from the period 1871 - 1900. In the 200 years of the  
12 CCSM3\_POP spin-up run, the simulated world ocean heat content in the upper 700m shows no  
13 sign of drift after about 150 years. Nevertheless, the 900 years of spin-up may not be long  
14 enough for deep oceans to reach a quasi-equilibrium state, if there is any. Therefore, to check  
15 and ensure that there is no long-term model drift in the real-time experiments to be described  
16 below, the CCSM3\_POP spin-up run is continued for additional 138 years, which is referred to  
17 as the reference experiment (EXP\_REF).

18 After the total of 900 years of spin-up runs, three model experiments are performed as  
19 summarized in Table S1. In the control experiment (EXP\_CTR), the CCSM3\_POP is integrated  
20 for 1871-2008 using the real-time daily 20CR surface flux fields. The next two experiments are  
21 idealized experiments designed to understand the Atlantic Ocean heat content change with and  
22 without the influence of the northward heat transport change at 30°S. The remote ocean warming  
23 experiment (EXP\_REM) is identical to EXP\_CTR except that the surface forcing fields north of

1 30°S are from the daily 20CR surface flux fields for the period of 1871-1900 exactly like  
2 EXP\_REF, whereas those south of 30°S are as in EXP\_CTR. Similar to EXP\_REM, the Atlantic  
3 Ocean warming experiment (EXP\_ATL) is also identical to EXP\_CTR except that the surface  
4 forcing fields south of 30°S are from EXP\_REF, whereas those north of 30°S are from  
5 EXP\_CTR. Note that the Atlantic Ocean warms only through anomalous surface heating in  
6 EXP\_ATL, and only through anomalous northward ocean heat transport at 30°S in EXP\_REM,  
7 respectively.

8

#### 9 **4. Results**

10 Figure 1a shows the time series of simulated Atlantic Ocean heat content in the upper 700 m  
11 in reference to the 1871-1900 baseline period obtained from the three model experiments, along  
12 with the observed heat content of the Atlantic Ocean. For a better visual comparison with the  
13 simulations, the observed heat content, which is recomputed from Levitus et al. [2009] for the  
14 Atlantic basin from 30°S to 75°N, is referenced in such a way that it matches the simulated heat  
15 content in EXP\_CTR averaged during 1955-1964. The simulated heat content of the Atlantic  
16 Ocean in EXP\_CTR increases moderately during the first half of the 20th century, after which it  
17 increases substantially. During the 1970s – 2000s, it increases by  $5 \sim 6 \times 10^{22}$  J. This large  
18 increase is reasonably close to the observed Atlantic Ocean heat content increase during the same  
19 period [Levitus et al., 2009]. In EXP\_ATL, the North Atlantic Ocean heat content increases by  
20 only  $\sim 2 \times 10^{22}$  J during the 1970s - 2000s; thus the local variable surface fluxes alone cannot  
21 explain the observed North Atlantic Ocean heat content increase. In EXP\_REM, on the other  
22 hand, the Atlantic Ocean heat content increases by  $3 \sim 4 \times 10^{22}$  J during the 1970s – 2000s  
23 explaining a large portion of the simulated trend in EXP\_CTR. The simulated Atlantic Ocean

1 heat content in EXP\_REF does not show any long-term model drift affirming that the increased  
2 Atlantic Ocean heat content in EXP\_CTR is not an artifact of the model simulation.

3 Figure 1b shows the heat budget terms for the Atlantic Ocean, obtained from EXP\_CTR,  
4 namely the southward heat transport for the entire water column at 75°N, the northward heat  
5 transport for the entire water column at 30°S, and the surface heat flux into the Atlantic Ocean  
6 between 30°S and 75°N, all referenced to the 1871-1900 baseline period. The simulated  
7 northward heat transport at 30°S is about 0.1 ~ 0.2 PW larger in the 1960s - 2000s period than in  
8 the earlier periods, consistent with the large Atlantic Ocean heat content increase in EXP\_CTR  
9 (Figure 1a). On the other hand, it is clear that both the surface heat flux and the northward  
10 Atlantic Ocean heat transport at 75°N have little impact on the Atlantic Ocean warming since the  
11 mid-20th century. Therefore, these model results fully support the hypothesis that the enhanced  
12 warming of the Atlantic Ocean since the mid-20th century is largely due to the increased ocean  
13 heat transport into the Atlantic basin across 30°S.

14

## 15 **5. AMOC Variability at 30°S**

16 Dong et al. [2009] showed that the northward heat transport in the South Atlantic near 30°S  
17 could be directly scaled with the AMOC strength. Therefore, the baroclinic volume transport  
18 (i.e., AMOC) in the South Atlantic at 30°S and its contribution to the large increase in the  
19 simulated ocean heat transport into the Atlantic basin is explored in this section.

20 Figure 2a shows the time-averaged AMOC during 1979-2008 obtained from EXP\_CTR. The  
21 simulated maximum strength of the AMOC at 35°N is only 11 Sv ( $1\text{Sv} = 10^6 \text{ m}^3\text{s}^{-1}$ ), which is  
22 smaller than the observed range of 14 ~ 20Sv. Increasing the vertical diffusivity in the model  
23 boosts the AMOC strength [e.g., Mignot et al. 2006]. However, since other model features



1 deteriorate with the increased vertical diffusivity, the vertical diffusivity is not increased in this  
2 study. Despite the smaller maximum strength, the overall spatial structure of the simulated  
3 AMOC is quite close to that derived from observations [e.g., Lumpkin and Spear 2007].

4 Figure 2b shows the time series of the simulated AMOC index (maximum overturning  
5 streamfunction) at 30°S. It clearly shows that the AMOC at 30°S increases after the 1940s,  
6 suggesting that the increased northward heat transport in the South Atlantic at 30°S (Figure 1b) is  
7 linked to the increased baroclinic volume transport at 30°S. The AMOC at 30°S in EXP\_REM  
8 has a similar increase as in EXP\_CTR (Figure S1a). On the other hand, the AMOC at 30°S in  
9 EXP\_ATL (Figure S1b) does not show a large long-term trend. These results strongly suggest  
10 that the processes within the Atlantic Ocean do not cause the increased AMOC strength at 30°S  
11 after the 1940s in EXP\_CTR. In other words, the AMOC increase at 30°S is pushed from the  
12 outside, rather than pulled from the inside.

13 The effect of the increased AMOC versus the increased upper ocean temperature in the South  
14 Atlantic at 30°S can be assessed by using the model output fields from EXP\_CTR. Using only  
15 the Eulerian-mean component of the meridional flow and the ocean temperature, we find that the  
16 purely thermal effect (i.e., only due to ocean temperature changes) accounts for about 20%  
17 increase of the heat transport at 30°S between 1871-1900 and 1979-2008 periods, whereas the  
18 purely dynamic effect (i.e., only due to meridional flow changes) accounts for more than 120%  
19 increase, clearly suggesting that the upper ocean thermal change of the inflow is insufficient to  
20 explain the large increase in the simulated ocean heat transport into the Atlantic basin.

21

## 22 **6. The Role of South Atlantic and Indian Subtropical Gyres**

1       The main conclusion so far is that the observed large warming of the Atlantic basin during  
2 the latter half of the 20th century is mainly due to the increased ocean heat transport into the  
3 Atlantic basin across 30°S, and that the anomalous northward ocean heat transport at 30°S is  
4 caused not only by the increased upper ocean temperature at 30°S but also, and more strongly, by  
5 the increased AMOC at 30°S.

6       Remote mechanical and thermal forcing appear to strengthen the AMOC and associated heat  
7 transport at 30°S. In order to understand the mechanisms, it is helpful to explore the simulated  
8 pathways of the northward heat transport in the Atlantic Ocean. Shown in Figure 3a are the  
9 simulated northward heat transport (contours) and heat transport vector averaged in the upper  
10 3000 m for 1979-2008, obtained from EXP\_CTR. It clearly shows that the main pathway of heat  
11 into the South Atlantic in this model originates in the Indian Ocean. The key roles played in  
12 global climate by the Indian-Atlantic inter-ocean exchange have long been recognized [e.g.,  
13 Biastoch et al., 2009; Beal et al., 2011]. The warm water that leaks from the Indian Ocean, the  
14 so-called Agulhas leakage, into the South Atlantic may affect the strength of the AMOC, both on  
15 decadal advective time scales and on faster Rossby wave time scales [e.g., Van Sebille and Van  
16 Leeuwen, 2007]. As shown in Figure 3a, the warm water leaked from the Indian Ocean moves  
17 northwestward along the South Atlantic subtropical gyre until it reaches the western boundary,  
18 then continues its northward excursion through the cross-hemispheric western boundary current  
19 system. The warm water finally arrives at the subpolar Atlantic via the Loop Current, Gulf  
20 Stream and North Atlantic Current, respectively. In reality most Agulhas leakage is carried by  
21 Agulhas rings, mesoscale features that are not well represented at this model's resolution [e.g.  
22 Beal et al., 2011 and references therein]. Nevertheless, the pathways of the heat transport shown

1 in Figure 3a are very similar to the advective pathways of mass seen in both high-resolution  
2 models and surface drifters [Van Sebille et al., 2011].

3 Figure 3b is identical to Figure 3a except that it shows the difference in the simulated  
4 northward heat transport (contours) and heat transport vector between 1979-2008 and 1871-1900  
5 periods. The pathways of the anomalous northward ocean heat transport are surprisingly similar  
6 to those of the mean northward ocean heat transport (Figure 3a). It is also clear that the inter-  
7 ocean heat transport from the Indian Ocean is increased. This agrees with recent studies in the  
8 Agulhas region, on the boundary between the Indian and Atlantic Oceans, which show an  
9 increase in both upper ocean temperature [Rouault et al., 2009] and inter-ocean transport  
10 [Biaostoch et al., 2009] in recent decades. The anomalous anticyclones of the barotropic stream  
11 function in the South Atlantic and Indian Ocean between 50°S and 30°S (Figure S2) further  
12 indicate that both the South Atlantic subtropical gyre and Indian Ocean subtropical gyre are  
13 strengthened. As shown in Figure 3c, this is consistent with the observed westerly wind  
14 anomalies over the Southern Ocean and the associated strengthening of the wind stress curl over  
15 the South Atlantic and Indian subtropical gyres, as suggested by earlier high- and low-resolution  
16 modeling studies [Biaostoch et al., 2009; Sijp and England, 2009]. Note that Ekman transport does  
17 not directly contribute to the increased AMOC at 30°S since the zonal wind stress at 30°S is  
18 nearly unchanged (Figure 3c). Since the westerly wind anomalies over the Southern Ocean are  
19 largely linked to the Southern Annular Mode (SAM), it appears that the increased AMOC at  
20 30°S in EXP\_CTR is ultimately caused by the increasing trend of the SAM since the mid-20th  
21 century. The cause of the SAM trend is not the focus of this study, but one popular hypothesis  
22 involves the Antarctic ozone losses with important contributions from anthropogenic  
23 chlorofluorocarbons [e.g., Thompson and Solomon, 2002].

1  
2  
3  
4  
5  
6  
7  
8  
9  
10  
11  
12  
13  
14  
15  
16  
17  
18  
19  
20  
21  
22  
23

## 7. Discussions

Obviously, there remain many crucial questions. One such question is the role of basin-scale low-frequency climate variability such as the Atlantic multidecadal oscillation (AMO) and the Pacific decadal oscillation on the differential inter-ocean warming. In particular, the AMO, which arguably results from the natural oscillation of the AMOC driven in the North Atlantic sinking regions [e.g., Knight et al., 2005; Lee and Wang, 2010], may have directly contributed to the rapid warming of the Atlantic Ocean since the 1950s. As shown in Figure S3a, the simulated North Atlantic Ocean heat content in EXP\_ATL exhibits a low-frequency multidecadal signal similar to the observed AMO, almost perfectly reproducing that of EXP\_CTR prior to the 1960s. In EXP\_REM, however, the multidecadal signal during the 1920s – 1950s, which is clearly visible in both EXP\_CTR and EXP\_ATL is completely missing. The absence of this multidecadal signal in EXP\_REM suggests that processes internal to the Atlantic Ocean cause the multidecadal swing in EXP\_CTR prior to the 1960s. During the 1960s – 2000s, on the other hand, remote processes seem to have contributed more than internal processes to the large increase in the North Atlantic heat content. The simulated South Atlantic Ocean heat content in EXP\_CTR and EXP\_REM is characterized by a monotonic increase after the 1960s, whereas in EXP\_ATL there is no apparent change in the South Atlantic heat content throughout the 20th century. These results lead to a conclusion that remote processes mainly forced the ocean heat content increase in both North and South Atlantic during the 1960s - 2000s in EXP\_CTR with a moderate contribution by internal processes in the North Atlantic.

There are some limitations in this study. In particular, the CCSM3\_POP used as the main tool in this study is not an eddy-resolving resolution model. Therefore, it is important that the

1 major findings of this study are further tested with higher resolution models. In particular, eddy-  
2 resolving resolution ( $\sim 0.1$  deg) models are required to properly simulate the role of eddies in the  
3 Agulhas leakage region [e.g., Beal et al. 2011]. A related issue is the eddy-driven heat and mass  
4 transports in the Southern Ocean, which are not well represented in this study.

5 A recent observational study [Böning et al. 2008] showed that the meridional overturning  
6 circulation in the Southern Ocean is insensitive to the intensification of Southern Hemisphere  
7 westerly winds over the past decades because the eddy-driven heat and mass transports largely  
8 compensate for the increased Ekman heat and mass transports in the Southern Ocean. Farneti and  
9 Delworth [2010] also showed that the AMOC change induced by changes in Southern  
10 Hemisphere westerly winds is much reduced in an eddy-resolving coupled climate model in  
11 comparison to that in a coarse-resolution model. Therefore, we acknowledge that the simulated  
12 AMOC increase at  $30^{\circ}\text{S}$  during the 1950s – 2000s could be an overestimate. Nevertheless, in our  
13 model simulation, the increased AMOC at  $30^{\circ}\text{S}$  is not directly forced by Ekman transport from  
14 the Southern Ocean because the zonal wind stress at  $30^{\circ}\text{S}$  is unchanged (Figure 3c). Instead, it is  
15 indirectly induced by the increased wind stress curl that strengthened the South Atlantic and  
16 Indian subtropical gyres and thus enhanced the inter-ocean volume transport from the Indian  
17 Ocean. A recent study that uses an eddy-resolving model indeed reported an increased volume  
18 transport from the Indian Ocean to the South Atlantic Ocean during the 1970s – 2000s [Biaosto  
19 et al., 2009], supporting the overall conclusions of this study.

20

21 **Acknowledgments.** We would like to thank the two anonymous reviewers for their thoughtful  
22 comments and suggestions, which led to a significant improvement of the paper. This study was  
23 motivated and benefited from the AMOC discussion group of the research community at

1 UM/RSMAS and NOAA/AOML. We wish to thank Igor Kamenkovich and all the participants  
2 who led the AMOC discussion group during the past year. We also acknowledge helpful  
3 suggestions from Ping Chang. This work is supported by the National Science Foundation (Grant  
4 No. 0850897).

5

6

### References

- 7 Barnett, T. P., D. W. Pierce, and R. Schnur (2001) Detection of anthropogenic climate change in  
8 the World's Oceans, *Science*, **292**, 270-274, doi:10.1126/science.1058304.
- 9 Barnett, T. P., D. W. Pierce, K. M. AchutaRao, P. J. Gleckler, B. D. Santer, J. M. Gregory, and  
10 W. M. Washington (2005) Penetration of human-induced warming into the World's Oceans,  
11 *Science*, **309**, 284-287, doi:10.1126/science.1112418.
- 12 Beal, L. M., W. P. M. De Ruijter, A. Biastoch, R. Zahn, and members of SCOR/ WCRP/IAPSO  
13 Working Group 136 (2011) On the role of the Agulhas system in ocean circulation and  
14 climate, *Nature*, **472**, 429-472, doi:10.1038/nature09983.
- 15 Biastoch, A., C. W. Böning, F. U. Schwarzkopf, and J. R. E. Lutjeharms (2009) Increase in  
16 Agulhas leakage due to poleward shift in the southern hemisphere westerlies, *Nature*, **462**,  
17 495-498, doi:10.1038/nature08519.
- 18 Böning, C. W., A. Dispert, M. Visbeck, S. R. Rintoul, and F. U. Schwarzkopf (2008) The  
19 response of the Antarctic Circumpolar Current to recent climate change, *Nat. Geosci.*, **1**, 864-  
20 869, doi:10.1038/ngeo362.
- 21 Broecker, W. S. (1987) The biggest chill, *Natural History*, **96**, 74-82.
- 22 Compo, G. P., and collaborators (2011) The twentieth century reanalysis project. *Quarterly J.*  
23 *Roy. Meteorol. Soc.*, **137**, 1-28. doi: 10.1002/qj.776.

1 Doney, S. C., Steve Yeager, G. Danabasoglu, W. G. Large, J. C. McWilliams (2007)  
2 Mechanisms governing interannual variability of upper-ocean temperature in a global ocean  
3 hindcast simulation. *J. Phys. Oceanogr.*, **37**, 1918–1938.

4 Dong, S., S. L. Garzoli, M. O. Baringer, C. S. Meinen and G. J. Goni (2009) Interannual  
5 variations in the Atlantic meridional overturning circulation and its relationship with the net  
6 northward heat transport in the South Atlantic. *Geophys. Res. Lett.*, **36**, L20606,  
7 doi:10.1029/2009GL039356.

8 Farneti, R., and T. L. Delworth (2010) The role of mesoscale eddies in the remote oceanic  
9 response to altered Southern Hemisphere winds. *J. Phys. Oceanogr.*, **40**,  
10 doi:10.1175/2010JPO4480.1.

11 Grist, J. P., and collaborators (2010) The roles of surface heat flux and ocean heat transport  
12 convergence in determining Atlantic Ocean temperature variability. *Ocean Dynam.*, **60**, 771-  
13 790, doi:10.1007/s10236-010-0292-4.

14 Knight, J. R., R. J. Allan, C. K. Folland, M. Vellinga, and M. E. Mann (2005) A signature of  
15 persistent natural thermohaline circulation cycles in observed climate, *Geophys. Res. Lett.*,  
16 **32**, L20708, doi:10.1029/2005GL024233.

17 Lee, S.-K. and C. Wang (2010) Delayed advective oscillation of the Atlantic thermohaline  
18 circulation, *J. Climate*, **23**, 1254-1261.

19 Lee, S.-K., D. B. Enfield and C. Wang (2011) Future impact of differential inter-basin ocean  
20 warming on Atlantic hurricanes, *J. Climate*, **24**, 1264-1275.

21 Levitus, S., J. I. Antonov, J. Wang, T. L. Delworth, K. W. Dixon, and A. J. Broccoli (2001)  
22 Anthropogenic warming of earth's climate system, *Science*, **287**, 2225-2229,  
23 doi:10.1126/science.287.5461.2225.

1 Levitus, S., J. I. Antonov, T. P. Boyer, R. A. Locarnini, H. E. Garcia, and A. V. Mishonov  
2 (2009) Global ocean heat content 1955–2008 in light of recently revealed instrumentation  
3 problems, *Geophys. Res. Lett.*, **36**, L07608, doi:10.1029/2008GL037155.

4 Lozier, M. S., V. Roussenov, S. Mark, C. Reed and R. G. Williams (2010) Opposing decadal  
5 changes for the North Atlantic meridional overturning circulation. *Nature Geosci.* **3**, 728-  
6 734.

7 Lumpkin, R. and K. Speer (2007) Global ocean meridional overturning. *J. Phys. Oceanogr.*, **37**,  
8 2550-2562.

9 Mignot, J., A. Levermann, and A. Griesel (2006) A decomposition of the Atlantic meridional  
10 overturning circulation into physical components using its sensitivity to vertical diffusivity.  
11 *J. Phys. Oceanogr.*, **36**, 636–650, doi: 10.1175/JPO2891.

12 Palmer, M. D., K. Haines, S. F. B. Tett, and T. J. Ansell (2007), Isolating the signal of ocean  
13 global warming, *Geophys. Res. Lett.*, **34**, L23610, doi:10.1029/2007GL031712.

14 Palmer M. D. and K. Haines (2009) Estimating oceanic heat content change using isotherms, *J.*  
15 *Climate*, **22**, 4953-4969.

16 Rouault, M., P. Penven, and B. Pohl (2009), Warming in the Agulhas Current system since the  
17 1980's, *Geophys. Res. Lett.*, **36**, L12, 602.

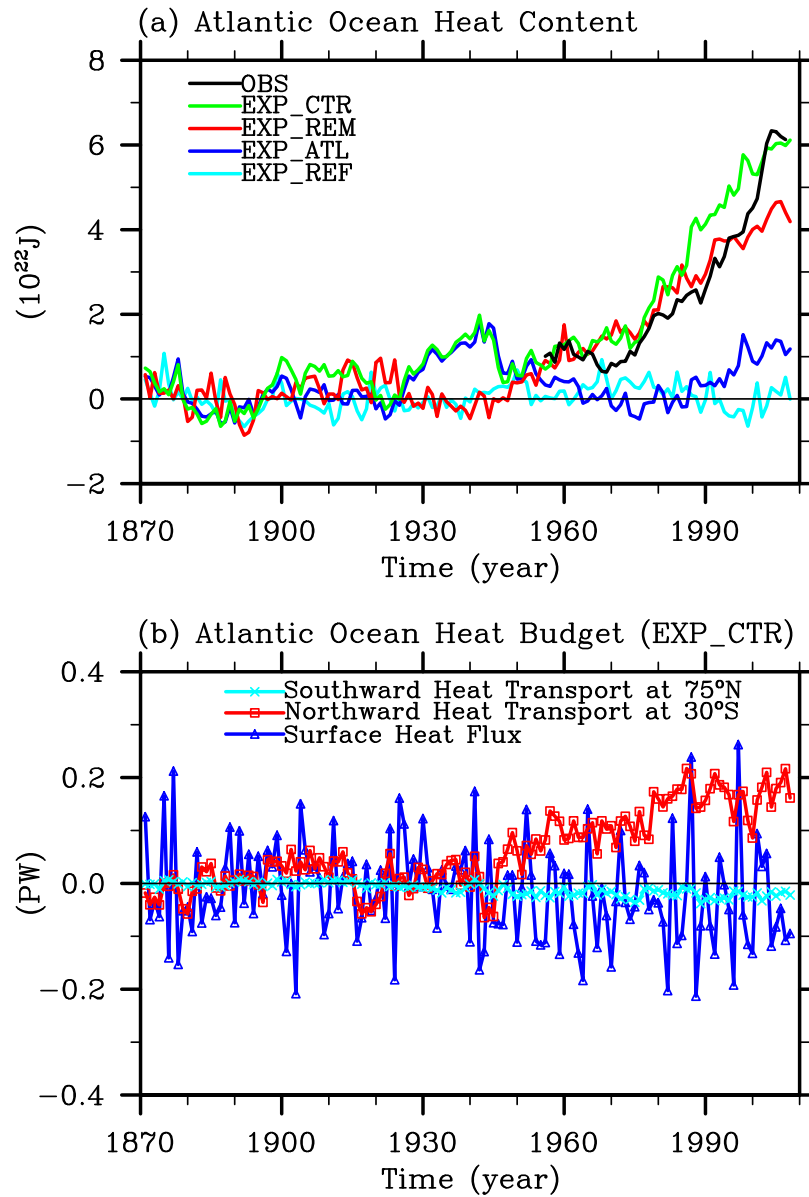
18 Sijp, W. P., and M. H. England (2009) Southern hemisphere westerly wind control over the  
19 ocean's thermohaline circulation. *J. Climate*, **22**, 1277-1286.

20 Thompson, D. W. and S. Solomon (2002) Interpretation of recent southern hemisphere climate  
21 change, 296, 895-899, doi:10.1126/science.1069270.

22 Van Sebille, E., and P. J. Van Leeuwen (2007) Fast northward energy transfer in the Atlantic due  
23 to Agulhas rings, *J. Phys. Oceanogr.*, **37**, 2305–2315.

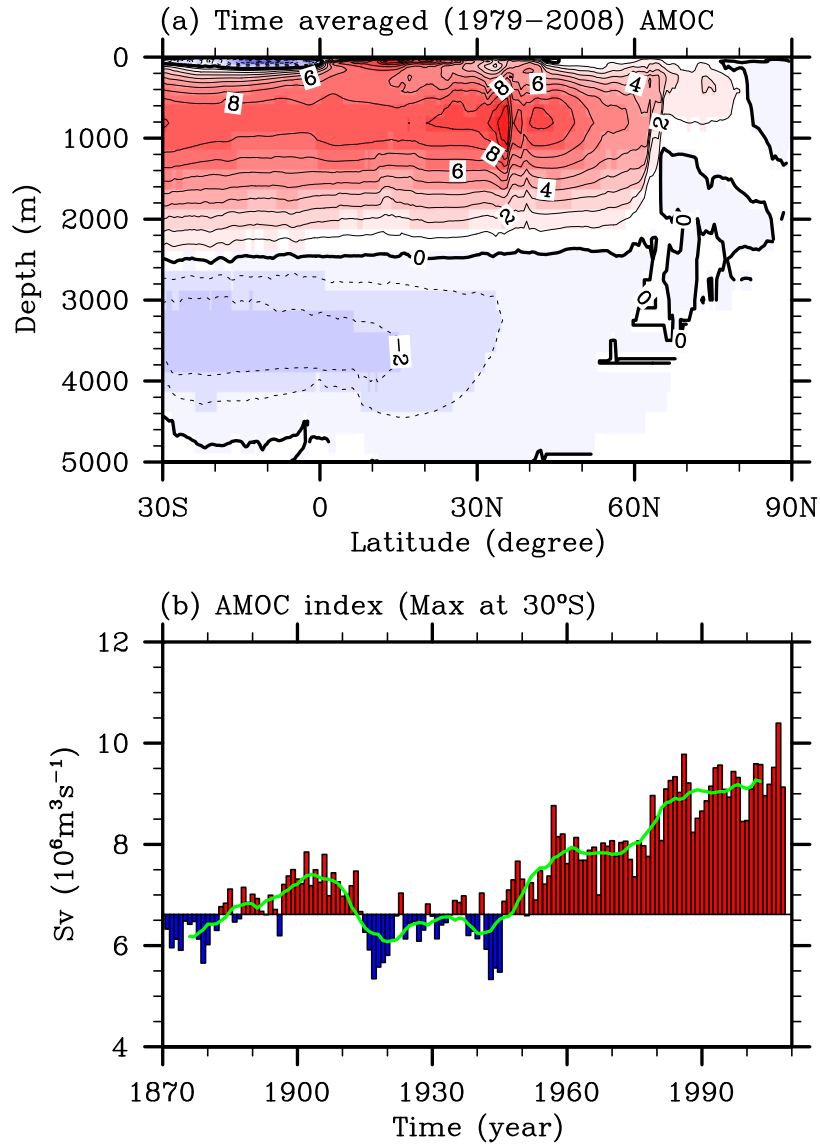


- 1 Van Sebille, E., L. M. Beal, and W. E. Johns (2011) Advective time scales of Agulhas leakage to
- 2 the North Atlantic in surface drifter observations and the 3D OFES model, *J. Phys.*
- 3 *Oceanogr.*, **41**, 1026-1034.



1  
 2 **Figure 1.** (a) Simulated Atlantic Ocean heat content change in the upper 700m in reference to  
 3 the 1871-1900 baseline period obtained from the four model experiments. The thick black line in  
 4 (a) is the observed heat content of the Atlantic Ocean, which is recomputed from Levitus et al.  
 5 [2009] for the Atlantic basin from 30°S to 75°N. (b) Simulated heat budget terms for the Atlantic  
 6 Ocean obtained from EXP\_CTR, all referenced to the 1871-1900 baseline period.

CCSM3\_POP (EXP\_CTR): AMOC



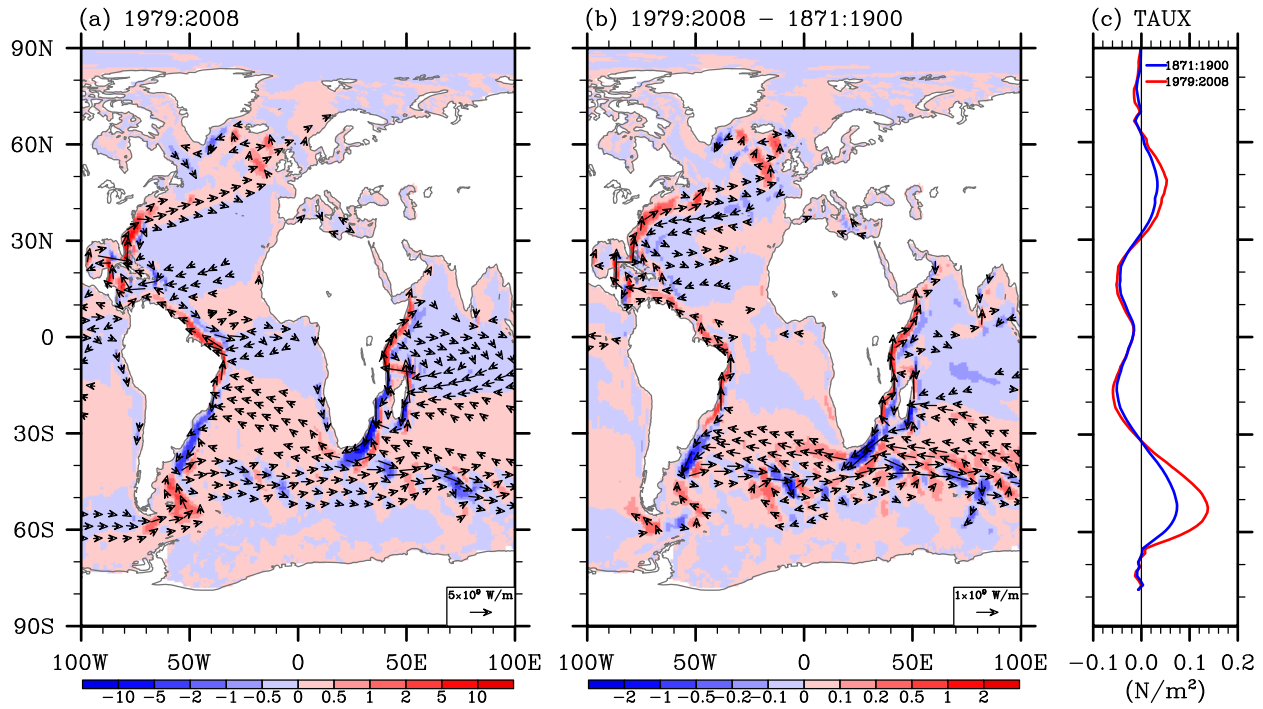
1

2 **Figure 2.** (a) Time-averaged AMOC during 1979-2008 and (b) time series of the simulated  
3 AMOC index (maximum overturning streamfunction) at 30°S obtained from EXP\_CTR. The  
4 green line in (b) is obtained by performing a 11- year running average to the AMOC index.

5

6

7



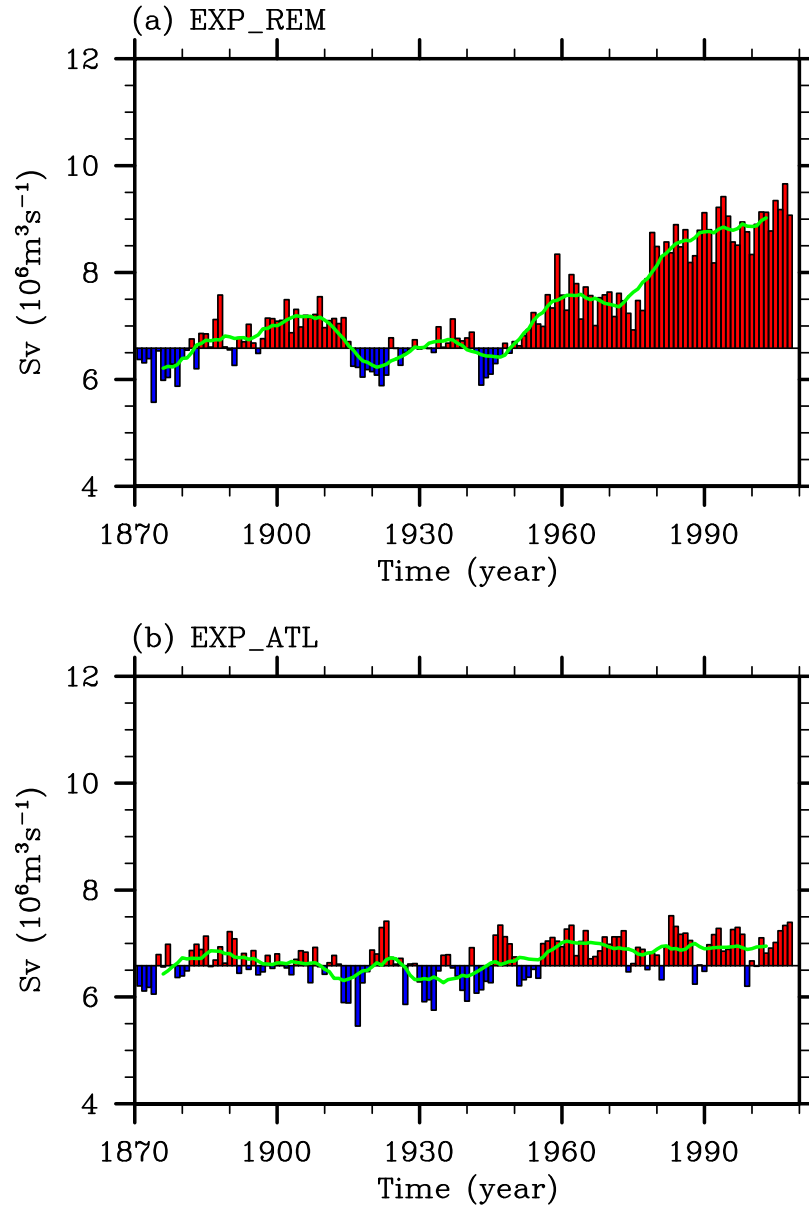
1  
 2 **Figure 3.** (a) Simulated pathways of the northward heat transport (contours) and heat transport  
 3 vector (vectors) in the upper 3000 m for 1979-2008 obtained from EXP\_CTR. The unit is  $1 \times 10^9$   
 4 W/m. (b) Differences in the simulated northward heat transport (contours) and heat transport  
 5 vector (vectors) between 1979-2008 and 1871-1900 periods, obtained from EXP\_CTR. Red  
 6 color indicates northward heat transport, while blue color indicates southward heat transport. (c)  
 7 Globally averaged zonal wind stress for 1871-1900 and for 1979-2008 periods, obtained from the  
 8 20CR.

1 Table S1. Summary of the surface forcing fields prescribed for the four model experiments.

Experiments	Surface Forcing Fields Prescribed
EXP_REF	Forced for 138 years with the forcing fields in each model year randomly selected from the 20CR forcing fields during 1871 – 1900.
EXP_CTR	Forced for 1871-2008 using the 20CR.
EXP_REM	Same as in EXP_CTR south of 30°S; Same as in EXP_REF north of 30°S
EXP_ATL	Same as in EXP_REF south of 30°S; Same as in EXP_CTR north of 30°S

2  
3  
4  
5  
6  
7  
8  
9  
10  
11  
12  
13  
14  
15  
16  
17

CCSM3\_POP: AMOC Index at 30°S



1

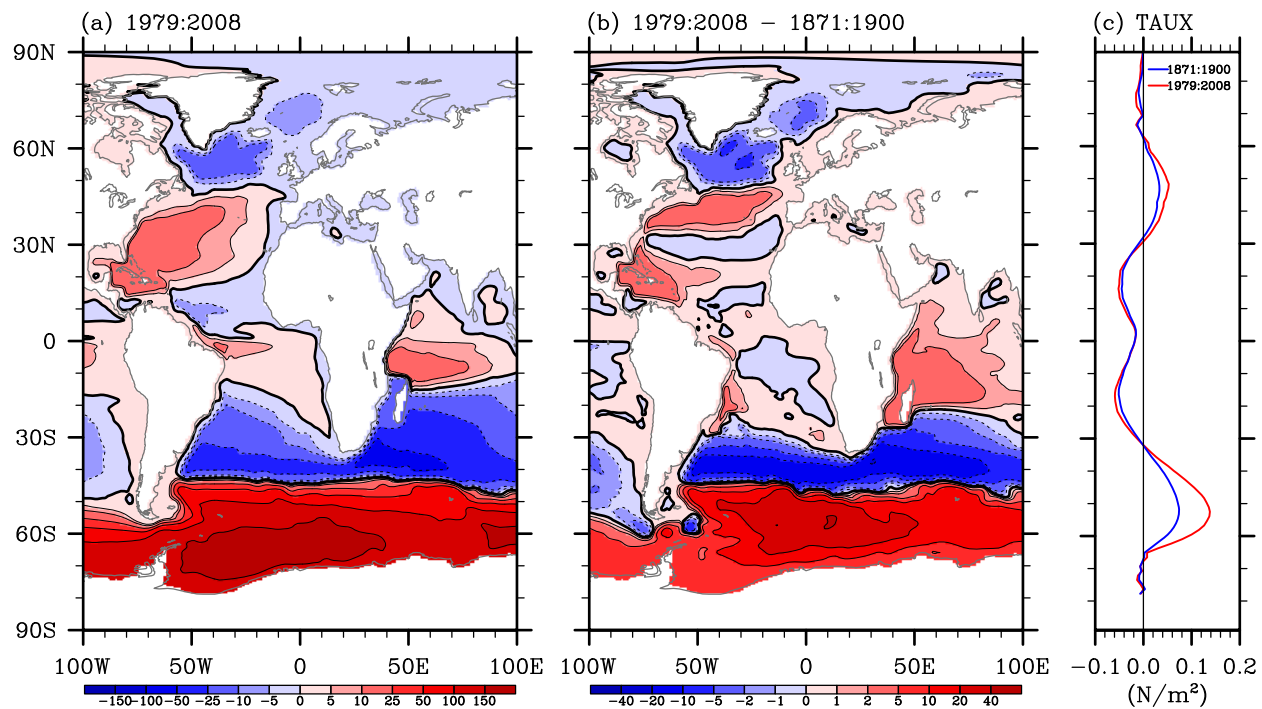
2 **Figure S1.** Time series of the simulated AMOC index (maximum overturning stream function)

3 at 30°S obtained from (a) EXP\_REM and (b) EXP\_ATL. Green lines are obtained by performing

4 a 11- year running average.

5

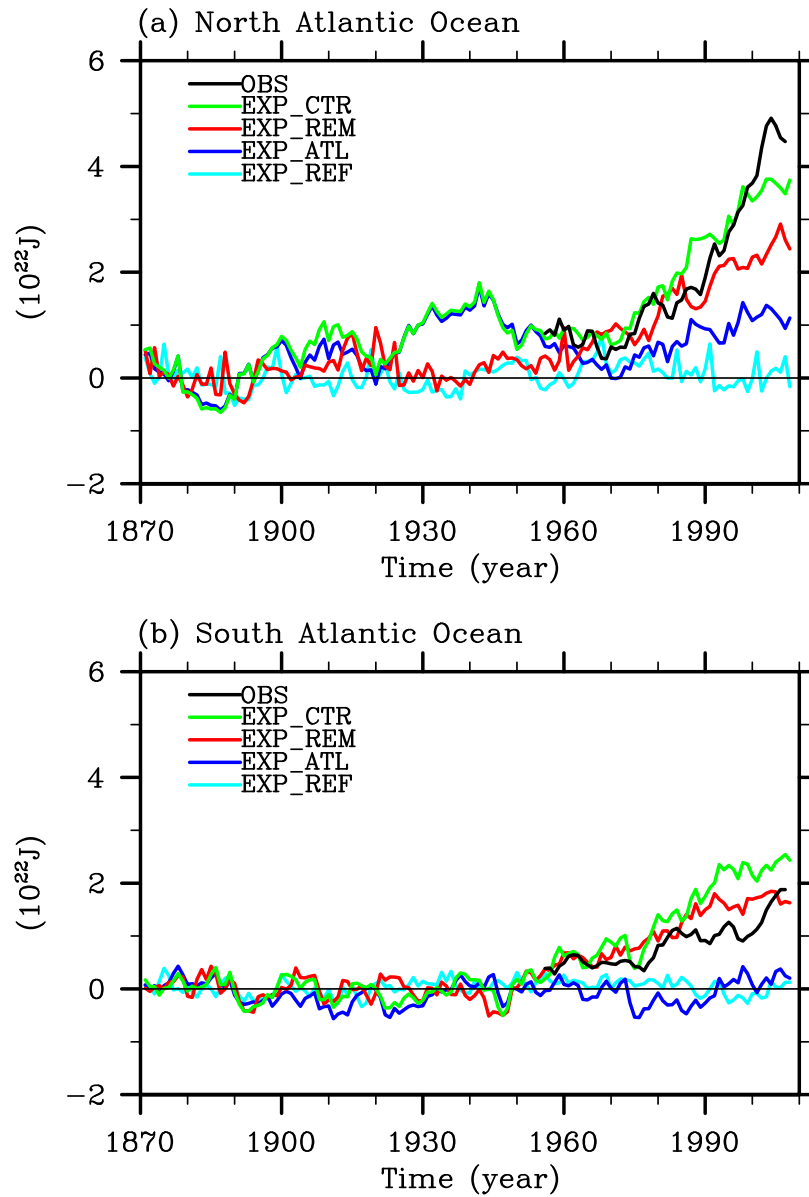
6



1  
 2 **Figure S2.** (a) Simulated barotropic streamfunction averaged for the 1979-2008 period obtained  
 3 from EXP\_CTR. (b) Difference in the simulated barotropic streamfunction between 1979-2008  
 4 and 1871-1900 periods, obtained from EXP\_CTR. The unit is Sv ( $10^6 m^3 s^{-1}$ ). (c) Globally  
 5 averaged zonal wind stress for 1871-1900 and for 1979-2008 periods, obtained from the 20CR.

6  
 7  
 8  
 9  
 10  
 11  
 12  
 13

CCSM3\_POP: ATL OCN Heat Content



1  
2 **Figure S3.** Simulated (a) North and (b) South Atlantic Ocean heat content changes in the upper  
3 700 m in reference to the 1871-1900 baseline period obtained from the four model experiments.  
4 The thick black lines in (a) and (b) are the observed heat contents recomputed from Levitus et al.  
5 [2009] for the North (equator -  $75^{\circ}\text{N}$ ) and South Atlantic ( $30^{\circ}\text{S}$  - equator), respectively.